ALGORITHM THEORETICAL BASIS DOCUMENT (ATBD) - QUANTUM LINE SENSOR

PREPARED BY	ORGANIZATION	DATE
Natchaya Pingintha-Durden	FIU	03/18/2013
Josh Roberti	FIU	09/28/2015
Derek Smith	FIU	01/07/2014
Hank Loescher	FIU	01/08/2013

APPROVALS	ORGANIZATION	APPROVAL DATE
Andrea Thorpe	SCI	10/23/2015
Dave Tazik	SCI	10/13/2015
Hanne Buur	PSE	10/20/2015

RELEASED BY	ORGANIZATION	RELEASE DATE
Jennifer DeNicholas	CM	10/23/2015

See configuration management system for approval history.

Change Record

REVISION	DATE	ECO #	DESCRIPTION OF CHANGE
A	08/28/2013	ECO-00980	Initial Release
B	10/23/2015	ECO-03110	Updated document to reflect L0 and L1 data product renumbering Revised *Algorithm Implementation* and *Uncertainty* Sections Implemented standardized coverage factor of k=2 Moved consistency analyses outline to Future Plans / Modifications Sections

TABLE OF CONTENTS

LIST OF TABLES AND FIGURES

1 DESCRIPTION

The LI-191-01 Quantum Line Sensor will be deployed in the soil array at NEON TIS sites to measure photosynthetically active radiation (PAR) at the soil surface. Contained in this document are details concerning PAR measurements made at all NEON sites. Specifically, the processes necessary to convert "raw" sensor measurements into meaningful scientific units and their associated uncertainties are described.

1.1 Purpose

This document details the algorithms used for creating NEON Level 1 (L1) data products (DP) from Level 0 data, obtained via instrumental measurements made by Licor LI-191-01 Quantum Line Sensor [NEON P/N: 0323440000]. It includes a detailed discussion of measurement theory and implementation, theoretical background, data product provenance, quality assurance and control methods used, assumptions, and a detailed estimation of uncertainty resulting in a cumulative uncertainty budget for this product.

1.2 Scope

This document describes the theoretical background and entire algorithmic process for creating L1 DPs from input data (L0). It does not provide computational methodology to implement the details of the approaches presented here, except for cases where they stem directly from algorithmic/mathematical choices explained here.

2 RELATED DOCUMENTS ACRONYMS AND VARIABLE NOMENCLATURE

2.1 Applicable Documents

AD[01]	NEON.DOC.000001	NEON OBSERVATORY
AD[02]	NEON.DOC.005003	NEON Scientific Data Products Catalog
AD[03]	NEON.DOC. 002652	NEON Level 1-3 Data Products Catalog
AD[04]	NEON.DOC.005005	NEON Level 0 Data Products Catalog
AD[05]	NEON.DOC.000782	ATBD QA/QC Data Consistency
AD[06]	NEON.DOC.011081	ATBD QA/QC plausibility tests
AD[07]	NEON.DOC.000783	ATBD De-spiking and time series analyses
AD[08]	NEON.DOC.000746	Evaluating Uncertainty (CVAL)
AD[09]	NEON.DOC.000603	NEON Sensor Command, Control, and Configuration - Quantum Line Sensor
AD[10]	NEON.DOC.000785	TIS Level 1 Data Products Uncertainty Budget Estimation Plan
AD[11]	NEON.DOC.000927	NEON Calibration and Sensor Uncertainty Values (CVAL)[1]
AD[12]	NEON.DOC.000752	Line Quanta PAR Calibration Fixture L2R400
AD[13]	NEON.FIU.011071	FIU Site Specific Sensor Location Matrix
AD[14]	NEON.DOC.001113	Quality Flags and Quality Metrics for TIS Data Products

2.2 Reference Documents

RD[01]	NEON.DOC.000008	NEON Acronym List
RD[02]	NEON.DOC.000243	NEON Glossary of Terms
RD[03]	LI-COR Terrestrial Radiation Sensors Instruction Manual	
RD[04]	LI-191SA Line Quantum Sensor Brochure	
RD[05]	Comparison of Quantum Sensors with Different Spectral Sensitivities, Technical Note #126	

2.3 Acronyms

Acronym	Explanation
ATBD	Algorithm Theoretical Basis Document
CI	NEON Cyberinfrastructure project team
CVAL	NEON Calibration, Validation, and Audit Laboratory
DAS	Data Acquisition System

[1] Note that CI obtains calibration and sensor values directly from an XML file maintained and updated by CVAL in real time. This report is updated approximately quarterly such that there may be a lag time between the XML and report updates.

DP	Data Product
FDAS	Field Data Acquisition System
FIU	Fundamental Instrument Unit
GRAPE	Grouped Remote Analog Peripheral Equipment
L0	Level 0
L1	Level 1
PAR	Photosynthetically Active Radiation
QA/QC	Quality Assurance/Quality Control
TIS	Terrestrial Instrument System

2.4 Variable Nomenclature

The symbols used to display the various inputs in the ATBD, e.g., calibration coefficients and uncertainty estimates, were chosen so that the equations can be easily interpreted by the reader. However, the symbols provided will not always reflect NEON's internal notation, which is relevant for Cyberinfrastructure's (CI's) use, and or the notation that is used to present variables on NEON's data portal. Therefore a lookup table is provided in order to distinguish what symbols specific variables can be tied to in the following document.

Symbol	Internal Notation	Description
C_1	CVALA1	CVAL calibration coefficient
u_{A1}	U_CVALA1	Combined, relative uncertainty of PAR sensor (%)
u_{A3}	U_CVALA3	Combined, relative uncertainty (truth and trueness only) of PAR sensor (%)
u_{V1}	U_CVALV1	Combined, relative uncertainty of Field DAS voltage measurements (%)
u_{V3}	U_CVALV3	Combined, relative uncertainty (truth and trueness only) of Field DAS voltage measurements (%)

2.5 Verb Convention

"Shall" is used whenever a specification expresses a provision that is binding. The verbs "should" and "may" express non-mandatory provisions. "Will" is used to express a declaration of purpose on the part of the design activity.

3 DATA PRODUCT DESCRIPTION

3.1 Variables Reported

PAR related L1 DPs provided by the algorithms documented in this ATBD are displayed in the accompanying file prq_datapub_NEONDOC002880.txt.

3.2 Input Dependencies

A summary of the inputs required to produce the Level 1 data product are shown in Table 3-1.

Table 3-1: The PAR related L0 DPs that are transformed into L1DPs in this ATBD.

Description	Sample Frequency	Units	Data Product Number
PAR sensor voltage (E_{out})	1 Hz	V	NEON.DOM.SITE.DP0.00066.001.01329.HOR.VER.000

3.3 Product Instances

Three quantum line sensors will be deployed at each site and shall reside within the soil plots.

3.4 Temporal Resolution and Extent

One- and thirty-minute averages of PAR at the soil surface will be calculated to form L1 DPs.

3.5 Spatial Resolution and Extent

The spatial resolution will depend on the placement of the quantum line sensor in the soil array. To maximize spatial coverage, one quantum line sensor per plot will be deployed in three out of five soil plots that comprise the soil array at each TIS site. Their measurements will be representative of the point in space where they are located. A description of how the sensors are located within plots is described in AD[13].

4 SCIENTIFIC CONTEXT

PAR is defined as radiation in the 400 nm to 700 nm waveband, which represents most of the visible solar radiation. This waveband is utilized directly by plant biochemical processes in photosynthesis to convert light energy into chemical energy, which is stored in the molecular bonds of organic molecules (e.g., sugars). PAR is also often referred to as Photosynthetic Photon Flux Density (PPFD), and estimated in quanta per unit area and per unit time, or µmol m^{-2} s^{-1}.

PAR measured via the quantum line sensor will provide information on the light availability at the ground level. This has significant ecophysiological applications as the light at the ground is patchy due to sunflecks, i.e., spots on the ground where direct (or near direct) solar radiation is incident. Many understory plants take advantage of these sunflecks through adaptation of their activation energy to charge the photosystems I and II (Jones, 1992; Salsbury and Ross 1978). While this ATBD describes the conversion of L0 to L1 data products, the data from the quantum line sensors is used in conjunction with the vertical profile of PAR sensors from the top to bottom of the tower structure. Ultimately, quantum line sensor data will inform higher-level data products and contribute to our understanding of energy balance and radiation transfer into and within the canopy. This will help to foster energy balance research by helping to answer various questions, such as how much radiation is attenuated or absorbed by the plant canopy and how much remains for biochemical processes.

4.1 Theory of Measurement/Observation

The LI-191-01 Quantum Line Sensor is designed for measuring PAR in applications where the solar radiation to be measured is spatially inhomogeneous, e.g., below plant canopies. Rather than using multiple detectors, the LI-191-01 uses a one meter long quartz rod under a diffuser to conduct light to a single high quantum sensor (RD[03]). The integrated horizontal measurement of PAR at the ground portrays a more representative measure than a single 'point' sensor.

The dashed black line in Figure 1 shows the ideal relative response of a quantum sensor in terms of sensitivity to photons: the sensor has no sensitivity (clear cutoffs) to light below 400 nm and above 700 nm, and a constant sensitivity to all photons across the 400 to 700 nm wavelength ranges. The sensitivity of the LI-191-01 (the solid green line in Figure 1) oscillates around the ideal quantum responses and has sharp cutoffs below 400 and above 700 nm (RD[05]). Output of the LI-191-01 is not biased significantly at either the blue or red ends of the spectrum. The actual area under each deviation from ideal is small and errors tend to cancel (RD[05]).

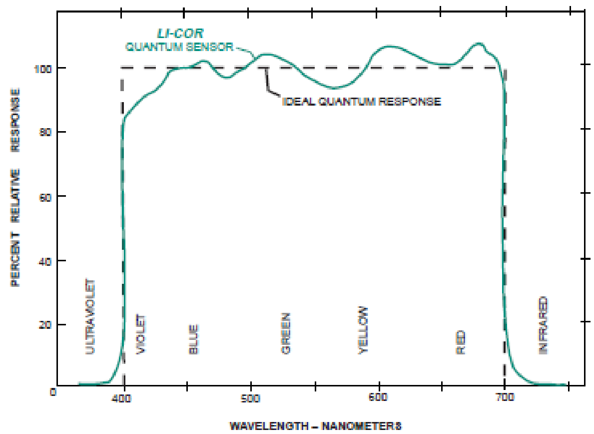

Figure 1. Relative spectral response of LI-191-01 quantum sensor (solid green line) and ideal quantum sensor (dashed black line). Source: RD[04].

4.2 Theory of Algorithm

The LI-191-01 sensor is a current output device. However, the current will be converted to voltage through a fixed resistor (1250 ohms, provided by NEON Engineering [ENG]) in the sensor which will require an independent calibration coefficient for each sensor. The calibration coefficient for each sensor will be determined by CVAL according to AD[12]. Using the sensor calibration coefficient and voltage output from the sensor, PAR is obtained in the required SI units (µmol m^{-2} s^{-1}) by:

$$PAR_i = C_1 * I_i \tag{1}$$

Where,

PAR_i = Individual (1 Hz) PAR at the soil surface (µmol m^{-2} s^{-1})

I_i = Individual LI-191-01 sensor output (V)

C_1 = LI-191-01 sensor calibration coefficient (µmol m^{-2} s^{-1} V^{-1}, provided by CVAL and sensor specific)

After PAR is determined, one-minute and thirty-minute averages of PAR will be determined according to Eq. (2) and (3) to create the L1 DPs listed in file prq_datapub_NEONDOC002880.txt. Individual calibrated measurements, i.e. 1 Hz PAR, will be made available upon request.

$$\overline{PAR_1} = \frac{1}{n}\sum_{i=1}^{n} PAR_i \tag{2}$$

where, for each 1-minute average, n is the number of measurements during the averaging period and PAR_i is a 1-Hz PAR measurement taken during the 60-second averaging period [0, 60). For a 1-minute average, n = 60 if all data points are included.

and

$$\overline{PAR}_{30} = \frac{1}{n}\sum_{i=1}^{n} PAR_i \tag{3}$$

where, for each 30-minute average, n is the number of measurements during the averaging period and PAR_i is a 1-Hz PAR measurement taken during the 1800-second averaging period [0, 1800).

Note: The beginning of the first averaging period in a series shall be the nearest whole minute less than or equal to the first timestamp in the series.

The third and fourth standardized moments of a random variable are known as the skewness and kurtosis of the random variable, respectively. The skewness is used as a measure of the asymmetry of the distribution and the kurtosis as a measure of the peakedness of the distribution. Together, sample estimates of these measures are often used to assess the normality of a distribution.

Both the skewness and the kurtosis will be estimated for one-minute and thirty-minute averaging periods of PAR as follows (NIST/SEMATECH, 2013):

$$\text{Skewness} = \frac{1}{(n-1)} \cdot \frac{\sum_{i=1}^{n}(PAR_i - \overline{PAR})^3}{s^3(PAR)} \tag{4}$$

And,

$$\text{Kurtosis} = \frac{1}{(n-1)} \cdot \frac{\sum_{i=1}^{n}(PAR_i - \overline{PAR})^4}{s^4(PAR)} \tag{5}$$

Where,

$$s(\text{PAR}) = \left(\frac{1}{(n-1)} \cdot \sum_{i=1}^{n}(PAR_i - \overline{PAR})^2\right)^{1/2} \tag{6}$$

is the standard deviation of PAR for either a one or thirty minute averaging period (µmol m^{-2} s^{-1}) and

$\overline{PAR}$	= One-minute or thirty-minute PAR average
n	= Number of measurements for a given one- or thirty-minute average

5 ALGORITHM IMPLEMENTATION

Data flow for signal processing of L1 data products will be treated in the following order.

1. 1 Hz data will be converted to PAR (µmol m^{-2} s^{-1}) using to Eq. (1) as described in section 4.2.
2. QA/QC Plausibility tests will be applied to the data stream in accordance with AD[06]. The details are provided below.
3. Signal de-spiking will be applied to the data stream in accordance with AD[07].
4. One- and thirty-minute PAR averages will be calculated using Eq. (2) and (3) and descriptive statistics (i.e. minimum, maximum, variance, skewness, and kurtosis) will be determined for both averaging periods.
5. Quality metrics, quality flags, and the final quality flag will be produced for one- and thirty-minute averages according to AD[14].

QA/QC Procedure:

1. **Plausibility Tests** AD[06] - All plausibility tests will be determined for PAR. Test parameters will be provided by FIU and maintained in the CI data store. Test parameters will be provided by FIU and maintained in the CI data store. All plausibility tests will be applied to the sensor's converted L0 DPs and associated quality flags (QFs) will be generated for each test.

2. **Signal De-spiking**– The time series de-spiking routine will be run according to AD[07]. Test parameters will be specified by FIU and maintained in the CI data store. Quality flags resulting from the de-spiking analysis will be applied according to AD[07].

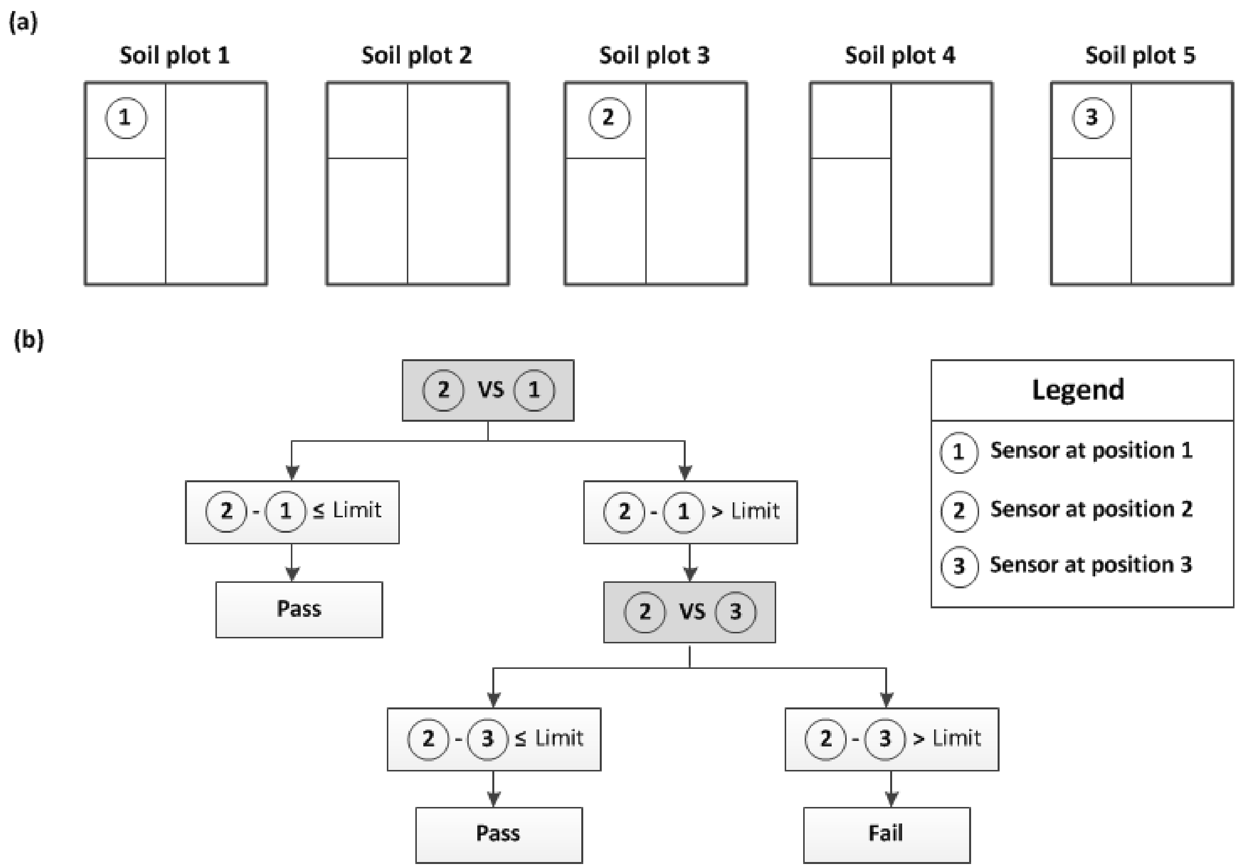

Figure 2. (a) Diagram of the position of the LI-191-01 sensors within the soil array and (b) consistency test flow diagram for the LI-191-01 sensor deployed at position 2.

3. **Quality Flags (QFs) and Quality Metrics (QMs)** AD[14] – If a datum has failed one of the following test it will not be used to create a L1 DP, range, persistence, and step α and β QFs and QMs will be determined using the flags listed in Table 5-1. In addition, L1 DPs will have a QA/QC report and quality metrics associated with each flag listed in Table 5-1 as well as a final quality flag (*finalQF*), as detailed in AD[14]. Ancillary information needed for the algorithm and other information maintained in the CI data store is shown in Table 5-2.

Table 5-1: Flags associated with the quantum line measurements.

Flags
Range
Persistence
Step

Null
Gap
Signal De-spiking
Alpha
Beta
Final Quality Flag

Table 5-2: Information maintained in the CI data store for the quantum line sensor.

Tests/Values	CI Data Store Contents
Range	Minimum and maximum values
Persistence	Window size, threshold values and maximum time length
Step	Threshold values
Null	Test limit
Gap	Test limit
Signal Despiking	Time segments and threshold values
Calibration	CVAL sensor specific calibration coefficients
Uncertainty	AD[11]
Consistency Analysis	Test limits
Final Quality Flag	AD[14]

6 UNCERTAINTY

Uncertainty of measurement is inevitable; therefore, measurements should be accompanied by a statement of their uncertainty for completeness (JCGM 2008; Taylor 1997). To do so, it is imperative to identify all sources of measurement uncertainty related to the quantity being measured. Quantifying the uncertainty of TIS measurements will provide a measure of the reliability and applicability of individual measurements and TIS data products. This portion of the document serves to identify, evaluate, and quantify sources of uncertainty relating to individual, calibrated PAR measurements as well as the L1 mean PAR DPs. It is a reflection of the information described in AD[12], and is explicitly described for the radiation assembly in the following sections.

6.1 Uncertainty of PAR Measurements

Uncertainty of the quantum line assembly is discussed in this section. The section is broken down into two topics. The first informs the sources of *measurement* uncertainty, i.e., those associated with *individual measurements*. The second details uncertainties associated with temporally averaged data products. A diagram detailing the data flow and known sources of uncertainty are displayed in Figure 3.

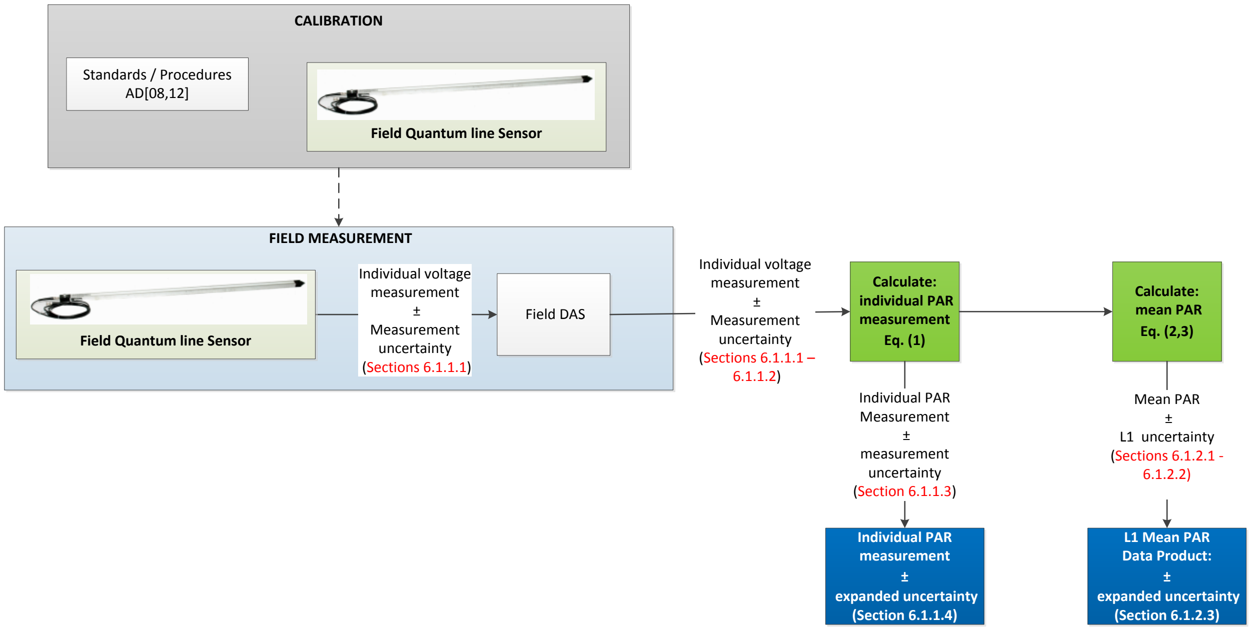

Figure 3. Displays the data flow and associated uncertainties of individual PAR measurements and L1 PAR DPs. For more information regarding the methods by which the PAR sensor is calibrated, please refer to AD[08, 12].

6.1.1 Measurement Uncertainty

The following subsections present the uncertainties associated with *individual PAR observations*. It is important to note that the uncertainties presented in the following subsections are *measurement uncertainties*, that is, they reflect the uncertainty of an *individual* PAR measurement. These uncertainties should not be confused with those presented in Section 6.1.2. We urge the reader to refer to AD[10] for further details concerning discrepancies between quantification of measurement uncertainties and L1 data product uncertainties.

NEON calculates measurement uncertainties according to recommendations of the Joint Committee for Guides in Metrology (JCGM) 2008. In essence, if a measurand *y* is a function of *n* input quantities x_i $(i = 1, \ldots, n)$, $i.e., y = f(x_1, x_2, \ldots, x_n)$, the combined measurement uncertainty of *y*, assuming the inputs are independent, can be calculated as follows:

$$u_c(y) = \left(\sum_{i=1}^{N} \left(\frac{\partial f}{\partial x_i} \right)^2 u^2(x_i) \right)^{\frac{1}{2}} \quad (7)$$

Where,

$\frac{\partial f}{\partial x_i}$ = partial derivative of *y* with respect to x_i

$u(x_i)$ = combined standard uncertainty of x_i.

Thus, the uncertainty of the measurand can be found be summing the input uncertainties in quadrature. For PAR measurements, the sources of uncertainty are depicted in 3. The calculation of these input uncertainties is discussed below.

6.1.1.1 Calibration

Uncertainties associated with the calibration process propagate into a combined, standard, measurement uncertainty. This uncertainty, u_{A1}, represents i) the repeatability and reproducibility of the sensor and the lab DAS and ii) uncertainty of the calibration procedures and coefficients including uncertainty in the standard (truth) (refer to Eq. (**1**). It is a relative value [%] that will be provided by CVAL (AD[11]) and stored in the CI data store. After converting from [%] to measurement units, it will be applied to all individual PAR measurements (that is, it does not vary with any specific sensor, DAS component, etc.). A detailed summary of the calibration procedures and corresponding uncertainty estimates can be found in AD[09,10,13].

The combined, standard, measurement uncertainty, $u_{CVAL}(PAR_i)$, is calculated as follows:

$$u_{CVAL}(PAR_i) = u_{A1} * PAR_i \tag{8}$$

6.1.1.2 Field DAS

The uncertainty introduced by the Field DAS (FDAS) through the voltage reading is:

$$u_{FDAS}(I_i) = (u_{V1} * I_i) + O_V \tag{9}$$

Where,

$u_{FDAS}(I_i)$ = combined, standard uncertainty of the voltage measurement introduced by the Field Das (V)

I = Sensor output (irradiance; V)

u_{V1} = combined, relative FDAS uncertainty for voltage measurements provided by CVAL (unitless)

O_V = offset imposed by the FDAS for voltage readings provided by CVAL (V)

The partial derivative of a PAR measurement with respect to the irradiance measurement is:

$$\frac{\partial PAR_i}{\partial I_i} = C_1; \tag{10}$$

therefore, the uncertainty of a PAR measurement due to the FDAS is:

$$u_{FDAS}(PAR_i) = \left|\frac{\partial PAR_i}{\partial I_i}\right| u_{FDAS}(I_i) \qquad (11)$$

Where,

$\frac{\partial PAR_i}{\partial I_i}$ = partial derivative of Eq.(**1**) with respect to I_i (µmol m^{-2} s^{-1} V^{-1})

C_1 = calibration coefficient provided by CVAL (µmol m^{-2} s^{-1} V^{-1})

$u_{FDAS}(PAR_i)$ = converted, combined, standard uncertainty introduced by the Field DAS (µmol m^{-2} s^{-1})

6.1.1.3 Combined Measurement Uncertainty

The combined, standard, measurement uncertainty for an individual PAR measurement, $u_c(PAR_i)$, is given in units of µmol m^{-2} s^{-1}and computed by summing the individual uncertainties in quadrature (Eq. (7)):

$$u_c(PAR_i) = \left(u_{CVAL}^2(PAR_i) + u_{FDAS}^2(PAR_i)\right)^{\frac{1}{2}} \qquad (12)$$

6.1.1.4 Expanded Measurement Uncertainty

The expanded measurement uncertainty is calculated as:

$$U_{95}(PAR_i) = k_{95} * u_c(PAR_i) \qquad (13)$$

Where,

$U_{95}(PAR_i)$ = expanded measurement uncertainty at 95% confidence (µmol m^{-2} s^{-1})

k_{95} = 2; coverage factor for 95% confidence (unitless)

6.1.2 Uncertainty of L1 Mean Data Product

The following subsections discuss uncertainties associated with temporally averaged, i.e., L1 mean, data products. As stated previously, it is important to note the differences between the *measurement uncertainties* presented in Section 6.1.1 and the uncertainties presented in the following subsections. The uncertainties presented in the following subsections reflect the uncertainty of a time-averaged mean value, that is, they reflect the uncertainty of a distribution of measurements collected under non-controlled conditions (i.e., those found in the field), as well as any uncertainties, in the form of *Truth* and *Trueness*, related to the accuracy of the field assembly.

6.1.2.1 Repeatability (natural variation)

To quantify the uncertainty attributable to random effects, the distribution of the individual measurements is used. Specifically, the *standard deviation of the mean (natural variation),* is computed. This value reflects the repeatability of insolation measurements for a specified time period:

$$u_{NAT}(\overline{PAR}) = \frac{s(PAR_i)}{\sqrt{n}} \quad (14)$$

Where,

$u_{NAT}(\overline{PAR})$ = standard error of the mean (natural variation) (µmol m^{-2} s^{-1})

$s(PAR_i)$ = experimental standard deviation of individual observations for the defined time period (µmol m^{-2} s^{-1})

n = number of observations made during the defined time period. (unitless)

6.1.2.2 Calibration

The uncertainty detailed here is similar to that described in Section 6.1.1.1. However, this combined, relative uncertainty, u_{A3}, does not account for i) individual sensor repeatability, or ii) the variation of sensors' responses over a population (reproducibility). This component of uncertainty estimates the uncertainty due to the accuracy of the instrumentation in the form of *Truth* and *Trueness*, a quantity which is not captured by the standard error of the mean. It is a relative value [%] that will be provided by CVAL (AD[11]) and stored in the CI data store. After converting to measurement units, the uncertainty will be applied to the *maximum* PAR value observed over the averaging period.

$$u_{CVAL(TT)}(\overline{PAR}) = u_{A3} * PAR_{MAX} \quad (15)$$

Where, the subscript "MAX" represents the index, i, where the *maximum*, combined, standard, measurement uncertainty of an individual PAR measurement is observed over a set (averaging period) of observations. Mathematically, this can be defined as:

$$MAX = \{i: u_c(T_i) = \max[u_c(PAR_1), \ldots, u_c(PAR_n)]\}. \quad (16)$$

And,

$u_{CVAL(TT)}(\overline{PAR})$ = combined, standard, Field DAS *Truth* and *Trueness* uncertainty due to the PAR measurement (µmol m^{-2} s^{-1})

PAR_{MAX} = PAR measurement corresponding to the maximum, combined, standard measurement uncertainty of PAR during the averaging period (µmol m^{-2} s^{-1})

u_{A3} = Combined, relative uncertainty (*Truth* and *Trueness* only) of PAR sensor (%)

Please refer to AD[12] for further justification regarding evaluation and quantification of using the maximum index for quantification of these L1 mean data product uncertainties.

6.1.2.3 Field DAS

Since the L1 mean DP is a function of the individual measurements, any measurement bias introduced by the Field DAS will be reflected in the L1 mean data product. Here, the raw measurement that maximizes the combined uncertainty of an individual measurement (Eq.(12)) is used in the calculation of the L1 mean DP uncertainty. Uncertainty components due to random effects, whether a function of the environment or the measurement assembly, are quantified via the natural variation of the mean (see Section 6.1.2.1). For more information regarding the justification of this approach, please see AD[12].

The accuracy of the Field DAS in the form of *Truth* and *Trueness* propagates through to the uncertainty of the mean DP similarly to how the Field DAS uncertainty associated with a raw resistance propagates through to the uncertainty of the measurement attributable to the Field DAS (Eqs. (9)-(11)).

$$u_{FDAS(TT)}(I_{MAX}) = (u_{V3} * I_{MAX}) + O_V \tag{17}$$

Where,

$u_{FDAS(TT)}(I_{MAX})$ = FDAS *Truth* and *Trueness* uncertainty of I_{MAX} (V)

I_{MAX} = individual irradiance measurement observed at MAX index (V)

u_{V3} = combined, relative, FDAS uncertainty (truth and trueness only) for voltage measurements; provided by CVAL (%)

O_V = offset imposed by the FDAS for voltage measurements provided by CVAL (V)

Thus, analogous to Eq. (11),

$$u_{FDAS(TT)}(\overline{PAR}) = \left|\frac{\partial PAR_i}{\partial I_i}\right|_{I_{MAX}} u_{FDAS(TT)}(I_{MAX}) \tag{18}$$

Where,

$\left|\frac{\partial PAR_i}{\partial I_i}\right|_{I_{MAX}}$ = partial derivative of PAR_i with respect to I_i (Eq. (10)) evaluated at I_{MAX} (µmol m^{-2} s^{-1} V^{-1})

C_1 = calibration coefficient provided by CVAL (µmol m^{-2} s^{-1} V^{-1})

$u_{FDAS(TT)}(\overline{PAR})$ = *Truth* and *Trueness* uncertainty of the mean DP introduced by the Field DAS (µmol m^{-2} s^{-1})

6.1.2.4 Combined Uncertainty

The combined uncertainty for our L1 mean PAR data product, $u_c(\overline{\mathrm{PAR}})$, given in units of µmol m^{-2} s^{-1}, is computed by summing the uncertainties from Sections 6.1.2.1 through 6.1.2.3 in quadrature:

$$u_c(\overline{\mathrm{PAR}}) = \left(u_{NAT}^2(\overline{PAR}) + u_{CVAL(TT)}^2(\overline{PAR}) + u_{FDAS(TT)}^2(\overline{PAR})\right)^{\frac{1}{2}} \quad (19)$$

6.1.2.5 Expanded Uncertainty

The expanded uncertainty is calculated as:

$$U_{95}(\overline{\mathrm{PAR}}) = k_{95} * u_c(\overline{\mathrm{PAR}}) \quad (20)$$

Where:

$U_{95}(\overline{\mathrm{PAR}})$ = expanded L1 mean data product uncertainty at 95% confidence (µmol m^{-2} s^{-1})

k_{95} = 2; coverage factor for 95% confidence (unitless)

6.1.3 Uncertainty Budget

The uncertainty budget is a visual aid detailing i) quantifiable sources of uncertainty, ii) means by which they are derived, and iii) the order of their propagation. Uncertainty values denoted in this budget are either derived within this document or are provided by other NEON teams (e.g., CVAL), and stored in the CI data store.

Table 6-1: Uncertainty budget for an individual PAR measurement. Shaded rows denote the order of uncertainty propagation (from lightest to darkest).

Source of measurement uncertainty	**Measurement uncertainty component $u(x_i)$**	**Measurement uncertainty value** $[\mu mol\ m^{-2}\ s^{-1}]$	$\frac{\partial f}{\partial x_i}$	$u_{x_i}(Y) \equiv \left\lvert\frac{\partial f}{\partial x_i}\right\rvert u(x_i)$ $[\mu mol\ m^{-2}\ s^{-1}]$

1 Hz PAR	$u_c(PAR_i)$	Eq. (12)	n/a	n/a
Sensor/calibration	$u_{CVAL}(PAR_i)$	Eq. (8)	1	Eq. (8)
Field DAS	$u_{FDAS}(I_i)$	Eq. (9) [V]	Eq. (10)	Eq. (11)

Table 6-2: Uncertainty budget for L1 mean PAR measurements. Shaded rows denote the order of uncertainty propagation (from lightest to darkest).

Source of uncertainty	**Uncertainty component $u(x_i)$**	**Uncertainty value** $[\mu mol\ m^{-2}\ s^{-1}]$	$\frac{\partial f}{\partial x_i}$	$u_{x_i}(Y) \equiv \left\|\frac{\partial f}{\partial x_i}\right\| u(x_i)$ $[\mu mol\ m^{-2}\ s^{-1}]$
L1 mean PAR	$u_c(\overline{PAR})$	Eq. (19)	n/a	n/a
Natural variation	$u_{NAT}(\overline{PAR})$	Eq. (14)	1	Eq. (14)
Sensor/calibration	$u_{CVAL(TT)}(\overline{PAR})$	Eq. (15)	1	Eq. (15)
Field DAS	$u_{FDAS(TT)}(\overline{PAR})$	Eq. (17) [V]	Eq. (10)	Eq. (18)

7 FUTURE PLANS AND MODIFICATIONS

Future system flags may be incorporated into the data stream. Additionally, individual calibrated and QA/QC measurements with their respective uncertainties may become a common data output in the future.

Details concerning the evaluation and quantification of Sensor and Field DAS drift will be added to the uncertainty section.

QA/QC tests may be expanded to include consistency analyses among similar measurement streams. A QA/QC flag for data consistency will be applied according to the redundancy analysis outlined in AD[05], and a pass/fail flag will be generated to reflect this analysis. Assume soil type and ground cover are the same among soil plots at a given site and assume that the position of sensors are located within the soil array as shown in the Figure 2(a). To evaluate PAR at the soil surface for consistency, L1 PAR from a given LI-191-01 quantum line sensor (a quantum line sensor at position 2) will first be compared to the LI-191-01 sensor at position 1. If a difference between the two PAR measurements is less than the defined limits (provided by FIU and maintained in the CI data store) then the sensor will have passed its consistency analysis. Alternatively, a PAR difference between the LI-191-01 sensors outside the defined limits will result in a failed test. A failed test between the sensors in position 1 and 2 will result in the LI-191-01 sensor at position 2 being compared to the sensor at position 3. If this too results in a failed test, then the LI-191-01 sensor will have failed the consistency test and be flagged as such (Figure 2(b)). If the LI-191-01 sensor fails the first test but passes the second then it will have passed the consistency test. This test structure helps to ensure that non-functional sensors (e.g., sensors that are faulty or due for service) do not bias the test, since a resulting failed test will allow the sensor to be compared to the other one. Accordingly, the sensors at position 1 and 3 will be first compared to the nearby sensor (sensor at position 2) and then to each other. L1 DPs that fail the Consistency Analysis will continue to be reported, but will have an associated failed flag that will be included in the QA/QC summary. Note that the evaluation procedures of PAR at the soil surface for consistency may not be applied if soil type and ground cover are not consistent amongst the soil plots.

8 BIBLIOGRAPHY

Joint Committee for Guides in Metrology (JCGM) (2008) Evaluation of measurement data – Guide to the expression of uncertainty in measurement. pp. 120.

JCGM (2012) International vocabulary of metrology – Basic and general concepts and associated terms (VIM). 3rd Edition. pp. 92

Jones, H.G., (1992) Plants and microclimate: a quantitative approach to environmental plant physiology. 2nd Ed. Cambridge University Press, Cambridge, UK.

NIST/SEMATECH. 2013. NIST/SEMATECH e-Handbook of Statistical Methods. Sec. 1.3.5.11 [Online]. Available: http://www.itl.nist.gov/div898/handbook/ [January, 2014].

Salisbury, F. B. & Ross, C. W. (1978) Plant Physiology. 2nd Ed. Wadsworth Publishing Company, Belmont, California, USA.

Taylor, J. R. (1997) An Introduction to Error Analysis: The Study of Uncertainties in Physical Measurements. University Science Books, Mill Valley, California. 2nd Ed. pp. 327.